ISSN 1674-1056
http://cpb.iphy.ac.cn
http://iopscience.iop.org/cpb
中国物理 B
Chinese Physics
中国物理
Chinese Physics B

Tunneling dynamics of bosons in the diamond lattice chain

Na-Na Chang(常娜娜), Ju-Kui Xue(薛具奎)

Citation: Chin. Phys. B . 2018, 27(10): 105203. **doi:** 10.1088/1674-1056/27/10/105203

Journal homepage: http://cpb.iphy.ac.cn; http://iopscience.iop.org/cpb

What follows is a list of articles you may be interested in

Dense pair plasma generation and its modulation dynamics in counter-propagating laser field

Wei-Yuan Liu(刘维媛), Wen Luo(罗文), Tao Yuan(袁韬), Ji-Ye Yu(余继晔), Min Chen(陈民)

Chin. Phys. B . 2018, 27(10): 105202. **doi:** 10.1088/1674-1056/27/10/105202

Tunneling dynamics of a few bosons with both two-and three-body interactions in a double-well potential

Na-Na Chang(常娜娜), Zi-Fa Yu(鱼自发), Ai-Xia Zhang(张爱霞), Ju-Kui Xue(薛具奎)

Chin. Phys. B . 2017, 26(11): 115202. **doi:** 10.1088/1674-1056/26/11/115202

Dynamics of laser beams in inhomogeneous electron—positron—ion plasmas

Cheng Li-Hong, Tang Rong-An, Du Hong-E, Xue Ju-Kui

Chin. Phys. B . 2015, 24(7): 075201. **doi:** 10.1088/1674-1056/24/7/075201

Spectral modulation and supercontinuum generation assisted by infrared femtosecond plasma grating

Liu Zuo-Ye, Sun Shao-Hua, Shi Yan-Chao, Ding Peng-Ji, Liu Qing-Cao, Liu Xiao-Liang, Ding Bao-Wei, Hu Bi-Tao

Chin. Phys. B . 2013, 22(7): 075204. **doi:** 10.1088/1674-1056/22/7/075204

Comparative investigation of resistance and ability to trigger high voltage discharge for single and multiple femtosecond filaments in air

Guo Kai-Min, Hao Zuo-Qiang, Lin Jing-Quan, Sun Chang-Kai, Gao Xun, Zhao Zhen-Ming

Chin. Phys. B . 2013, 22(3): 035203. **doi:** 10.1088/1674-1056/22/3/035203

Tunneling dynamics of bosons in the diamond lattice chain*

Na-Na Chang(常娜娜) and Ju-Kui Xue(薛具奎)†

College of Physics and Electronics Engineering, Northwest Normal University, Lanzhou 730070, *China*

(Received 27 June 2018; revised manuscript received 2 August 2018; published online 10 September 2018)

We analyze the effect of tilting and artificial magnetic flux, on the energy bands structure for the system and the corresponding tunneling dynamics for bosons with various initial configurations in the diamond lattice chain, where intriguing and significant phenomena occur, including Landau–Zener tunneling, Bloch oscillations, and localization phenomenon. Both vertical tilting and artificial magnetic flux may alter the structure of energy levels (dispersion structure or flat band), and enforce the occurrence of Landau–Zener tunneling, which scans the whole of the Bloch bands. We find that, transitions among Landau–Zener tunneling, Bloch oscillations, and localization phenomenon, are not only closely related to the energy bands structure, but also depends on the initial configuration of bosons in the diamond lattice chain. As a consequence, Landau–Zener tunneling, Bloch oscillations, and localization phenonmenon of bosons always counteract and are complementary with each other in the diamond lattice chain.

Keywords: Bose–Einstein condensate, Landau–Zener tunneling, Bloch oscillation, localization, flat band

PACS: 52.27.Ep, 52.38.Hb, 98.70.Rz **DOI:** 10.1088/1674-1056/27/10/105203

1. Introduction

One of the most fundamental quantum effects is the tunneling phenomenon,[1–4] i.e., the transition of the particle between potential barrier, which is incapable of depicting by classical physics. Investigations concerning Landau–Zener tunneling and Bloch oscillations[5–8] have been advanced by the first experimental realization of Bose–Einstein condensation (BEC) in an optical lattice,[9–13] which provides a good opportunity for manipulating the tunneling dynamics in various optical lattices. A simple and straightforward description for the nonadiabatic transition between different Bloch energy levels is by the means of Landau–Zener tunneling.[8] Three-state systems are ubiquitously obtained, and this problem has been studied in various quantum systems, e.g., optical systems,[14,15] bosonic systems,[16–18] and Zener breakdown with metal–insulator transitions of semiconductors.[19–23] In particular, direct experimental observation of the Landau–Zener tunneling of BEC in an optical lattice[24,25] has been performed for the range of the potential amplitudes extended until several recoil energies (a deep optical lattice). Landau–Zener tunneling, Bloch oscillations, and localization phenonmenon for bosons can be induced by tilting of the optical lattice in the gravitational field[10] (or accelerating the whole lattice[24]) as well as the artificial magnetic field.[26–28]

As a prototype system to study interference and tunneling in great detail, a diamond lattice chain is one of the best candidates.[29–34] Subsequently, numerous theoretical efforts have been made to depict and further have a good understanding of a host of diverse and interesting phenomena in diamond lattice chain, including Landau–Zener tunneling, Bloch oscillations, and localization phenomenon, which skips different ranges of lattice sites in a single chain or among different chains. In particular, flat band and the corresponding compact localized state (CLS) are revealed in the diamond lattice chain of the BEC system.[32,34] The flat band is a dispersionless energy band composed of entirely degenerate states. Being the eigenstates of the flat band, CLS explicitly depicts flat band lattices,[35] which have nonzero amplitudes only on a finite number of sites.

The structure of energy levels for the diamond lattice chain can be altered by relevant parameter(s), thus, the tunneling dynamics exhibits novel and interesting quantum phenomena, which should also closely depend on the initial configurations of bosons in the system, however, it is still a problem to be solved in the diamond lattice chain at present. This paper investigates the effect of tilting and artificial magnetic flux, on the energy bands structure for the system and the corresponding tunneling dynamics for bosons with various initial configurations in the diamond lattice chain. It is found that the position of the minimum band gap for the crossing can be affected by the tilting of the diamond lattice chain and artificial magnetic flux within a single diamond plaquette. Hence, it may be possible to manipulate transitions among serval intriguing and novel quantum effects, including Landau–Zener tunneling, Bloch oscillations, and localization phenomenon, which also depends on the initial configurations of the bosons in the diamond lattice chain.

The paper is structured as follows. Section 2 introduces

*Project supported by the National Natural Science Foundation of China (Grant Nos. 11764039, 11475027, 11865014, 11865014, 11274255, and 11305132), the Natural Science Foundation of Gansu Province, China (Grant No. 17JR5RA076), and the Scientific Research Project of the Higher Education of Gansu Province, China (Grant No. 2016A-005).

†Corresponding author. E-mail: xuejk@nwnu.edu.cn

© 2018 Chinese Physical Society and IOP Publishing Ltd

our model and briefly reviews the computational method. Following a brief recapitulation for the energy bands structure of the system is given in Section 3. Section 4 gives a presentation of the tunneling dynamics for bosons with certain initial configurations in the diamond lattice chain. Ultimately, we present our conclusions in Section 5.

2. Model and method

We consider the tunneling dynamics of non-interacting Bose gas (that can be manipulated by the Feshbach technique) in one-dimensional diamond lattice chain as shown in Fig. 1. The various tunneling of bosons, along the same chain (Bloch oscillation) or among different chains (Landau–Zener tunneling), can be demonstrated by the following tight-binding model,[30]

$$\begin{aligned}\hat{H} =& \sum \varepsilon_{\rm v}(\hat{a}_n^{\dagger}\hat{a}_n - \hat{c}_n^{\dagger}\hat{c}_n) \\ &+ \varepsilon_{\rm h} n(\hat{a}_n^{\dagger}\hat{a}_n + \hat{b}_n^{\dagger}\hat{b}_n + \hat{c}_n^{\dagger}\hat{c}_n) + \frac{\varepsilon_{\rm h}}{2}\hat{b}_n^{\dagger}\hat{b}_n \\ &- [(\hat{b}_n^{\dagger}\hat{a}_n + \hat{c}_n^{\dagger}\hat{b}_n)\,{\rm e}^{{\rm i}\phi} - \hat{b}_{n-1}^{\dagger}\hat{c}_n - \hat{a}_n^{\dagger}\hat{b}_{n-1} + {\rm c.c.}], \quad (1)\end{aligned}$$

where a, b, and c index the three lattice sites of the diamond lattice chain, the yellow shadow rectangle defines the n-th unit cell of the diamond lattice chain, and n is the corresponding cell number. $\hat{a}_j^{\dagger}$, $\hat{b}_j^{\dagger}$, $\hat{c}_j^{\dagger}$ and $\hat{a}_j$, $\hat{b}_j$, $\hat{c}_j$ ($j = 1,2,\ldots,N$) are the creation and annihilation operators, respectively. The particles number operator is $\hat{n} = \hat{\psi}^{\dagger}\hat{\psi}$ ($\psi = a$, b, c), while $N = \hat{a}_n^{\dagger}\hat{a}_n + \hat{b}_n^{\dagger}\hat{b}_n + \hat{c}_n^{\dagger}\hat{c}_n$ denotes the total number of bosons in single diamond plaquette, which is a dynamical invariant of the system described by Eq. (1), along with the normalization condition $\sum_{n=0}^{N}(|a_n|^2 + |b_n|^2 + |c_n|^2) = 1$ in the whole diamond lattice chain. Note that c.c. stands for the complex conjugate expression. $\varepsilon_{\rm h}$ and $\varepsilon_{\rm v}$ describe the horizontal and vertical tilting while the artificial magnetic field (ϕ is the magnetic flux in a single plaquette) is denoted by B, which could detune the on-site energies of the network. Experimentally, the horizontal tilting $\varepsilon_{\rm h}$ and vertical tilting $\varepsilon_{\rm v}$ can be realized directly in the gravitational field[10] or accelerating the whole lattice,[24] while the magnetic field B can be generated by the means of artificial gauge fields.[26]

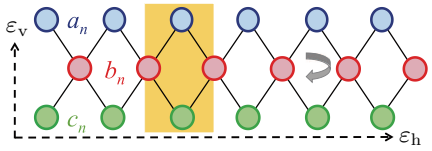


Fig. 1. (color online) The schematic of the diamond lattice chain with three legs, a (blue), b (red), and c (green). Note that $\varepsilon_{\rm h}$ and $\varepsilon_{\rm v}$ define the horizontal and vertical tilting while the artificial magnetic field B with the magnetic flux ϕ in a single plaquette (black solid arrows), which is perpendicular to the lattice plane. Lattice sites are designated by the circles with colored solid lines; simply black solid lines indicate sites concerning tunneling of bosons along diverse paths of diamond lattice chain; the yellow shadow rectangle defines the n-th unit cell of the diamond chain, which covers a (blue), b (red), and c (green) sites.

Based on the canonical transformation, i.e., ${\rm i}\hbar{\rm d}\hat{a}_n/{\rm d}t = \partial\hat{H}/\partial\hat{a}_n^*$, ${\rm i}\hbar{\rm d}\hat{b}_n/{\rm d}t = \partial\hat{H}/\partial\hat{b}_n^*$, ${\rm i}\hbar{\rm d}\hat{c}_n/{\rm d}t = \partial\hat{H}/\partial\hat{c}_n^*$ (here $\hbar = 1$), the corresponding discrete Schrödinger equations related to $a(n)$, $b(n)$, and $c(n)$ can be derived from Eq. (1) and read explicitly,

$$\begin{aligned}{\rm i}\frac{{\rm d}a_n}{{\rm d}t} &= (\varepsilon_{\rm h} n + \varepsilon_{\rm v})a_n - {\rm e}^{-{\rm i}\phi}b_n - b_{n-1}, \\ {\rm i}\frac{{\rm d}b_n}{{\rm d}t} &= \varepsilon_{\rm h}(n+\frac{1}{2})b_n - {\rm e}^{{\rm i}\phi}a_n - {\rm e}^{-{\rm i}\phi}c_n - c_{n+1} - a_{n+1}, \\ {\rm i}\frac{{\rm d}c_n}{{\rm d}t} &= (\varepsilon_{\rm h} n - \varepsilon_{\rm v})c_n - {\rm e}^{{\rm i}\phi}b_n - b_{n-1}, \quad (2)\end{aligned}$$

which are obtained from the mean-field approximation, i.e., $a_n \equiv \langle\hat{a}_n\rangle$, $b_n \equiv \langle\hat{b}_n\rangle$, $c_n \equiv \langle\hat{c}_n\rangle$, respectively.

In the absence of the horizontal tilting $\varepsilon_{\rm h}$, i.e., $\varepsilon_{\rm h} = 0$, the plane wave solution

$$\begin{aligned}a_n &= a(t)\,{\rm e}^{{\rm i}kn}({\rm e}^{-{\rm i}k} + {\rm e}^{-{\rm i}\phi}), \\ b_n &= b(t)\,{\rm e}^{{\rm i}kn}, \\ c_n &= c(t)\,{\rm e}^{{\rm i}kn}({\rm e}^{-{\rm i}k} + {\rm e}^{{\rm i}\phi}). \quad (3)\end{aligned}$$

holds, where k is the momentum of the bosons. The amplitudes of $a(t)$, $b(t)$, and $c(t)$ are satisfied with the equation, i.e.,

$${\rm i}\frac{\rm d}{{\rm d}t}\begin{pmatrix} a \\ b \\ c \end{pmatrix} = \begin{pmatrix} \varepsilon_{\rm v} & -1 & 0 \\ R & 0 & S \\ 0 & -1 & -\varepsilon_{\rm v} \end{pmatrix}\begin{pmatrix} a \\ b \\ c \end{pmatrix}, \quad (4)$$

where $R = -2[1+\cos(k-\phi)]$ and $S = -2[1+\cos(k+\phi)]$. The cubic equation concerning the eigenvalue $\lambda(k)$ is as an acquisition of exactly diagonalizing the Hermitian coefficient matrix for Eq. (4), i.e.,

$$\lambda^3 + (R + S - \varepsilon_{\rm v}^2)\lambda + (R - S)\varepsilon_{\rm v} = 0. \quad (5)$$

It is inconvenient to solve the cubic equation. As a consequence, the eigenvalue $\lambda(k)$ and the ground state solution $\{a(t), b(t), c(t)\}$ hold in the following special cases, i.e., when

$$\phi = 0, \quad \lambda_{\rm flat} = 0, \quad \lambda_{\pm} = \pm\sqrt{\varepsilon_{\rm v}^2 + 4(1+\cos k)}, \quad (6)$$

its corresponding CLS for $\lambda_{\rm flat} = 0$ is

$$\{a(t), \quad b(t), \quad c(t)\} = \{1, \varepsilon_{\rm v}, -1\}, \quad (7)$$

and the eigenstates for $\lambda_{\pm} = \pm\sqrt{\varepsilon_{\rm v}^2 + 4(1+\cos k)}$ are

$$\begin{aligned}&\{a(t), b(t), c(t)\} \\ &= \{[-2(1+\cos k) - \varepsilon_{\rm v}^2 \pm \varepsilon_{\rm v}\sqrt{4(1+\cos k) + \varepsilon_{\rm v}^2}]/2(1+\cos k), \\ &\quad \varepsilon_{\rm v} \mp \sqrt{4(1+\cos k) + \varepsilon_{\rm v}^2}, -1\}. \quad (8)\end{aligned}$$

When

$$\varepsilon_{\rm v} = 0 : \lambda_{\rm flat} = 0, \lambda_{\pm} = \pm 2\sqrt{1 + \cos\phi\cos k}, \quad (9)$$

its corresponding CLS for $\lambda_{\text{flat}} = 0$ is

$$\begin{aligned} &\{a(t), b(t), c(t)\} \\ &= \{[1+\cos(k+\phi)]/[1+\cos(k-\phi)], 0, -1\}, \end{aligned} \tag{10}$$

and the eigenstates for $\lambda_{\pm} = \pm 2\sqrt{1+\cos\phi\cos k}$ are

$$\begin{aligned} &\{a(t), b(t), c(t)\} \\ &= \{1, \pm\sqrt{2}\sqrt{2+\cos(k-\phi)+\cos(k+\phi)}, 1\}. \end{aligned} \tag{11}$$

Three branches of eigenvalue hold in each sample. It all comes non-flat other than the two specific cases, i.e., flat band only occurs in the two special cases,[31] however, other parameters of vertical tilting ε_{v} and artificial magnetic flux ϕ can also generate flat band, whose energy band dispersion relation as well as the counterparts of tunneling dynamics in the diamond chain will be shown later.

3. Energy band structure of the system

Solving Eq. (5) numerically, we find that, the energy bands can be fine-tuned by manipulating the parameters of vertical tilting ε_{v} and artificial magnetic flux ϕ in the diamond lattice chain, which is summarized in Figs. 2 and 3.

Here we first pay attention to the influence of the vertical tilting ε_{v} on the energy levels for the system with $\phi = 0$ (see Fig. 2). Energy bands cross at $k = \pm\pi$ when ε_{v} is absent ($\varepsilon_{\text{v}} = 0$), which can be seen in Fig. 3(a). As the increase of ε_{v} (the specific parameters as shown in Figs. 2(a), 2(b), and 2(c), respectively), the energy gap between λ_+ (blue line) and λ_- (black line) gradually enlarges (see Figs. 2(a), 2(b), and 2(c)), λ_+ and λ_- eventually become flat band as the further increase of ε_{v} ($\varepsilon_{\text{v}} = 10$), whose width of the energy gap is the maximum (see Fig. 2(d)), therefore, three flat bands ($\lambda_{\text{flat}} = 0$, $\lambda_{\pm} = \pm 10$) hold when $\varepsilon_{\text{v}} = 10$, whose CLS is as Eq. (7).

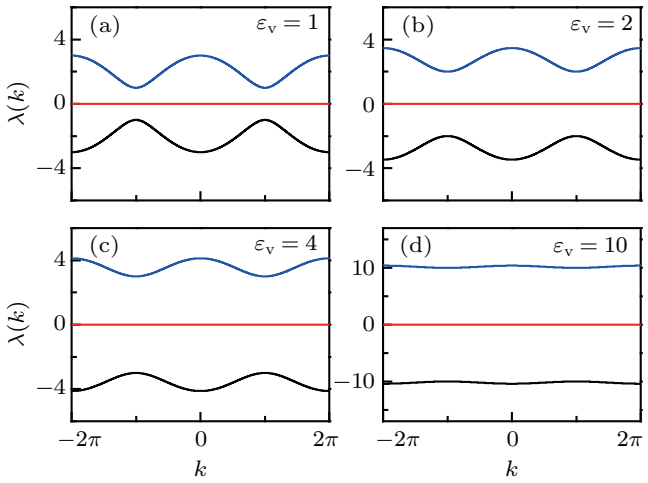


Fig. 2. (color online) Energy band $\lambda(k)$ versus wave number k for different vertical tilting ε_{v} with the synthetic magnetic flux $\phi = 0$, which contains a flat band λ_{flat} (red line) and two non-flat bands $\lambda_{\pm}$ (blue and black lines). Note that the horizontal tilting $\varepsilon_{\text{h}} = 0$.

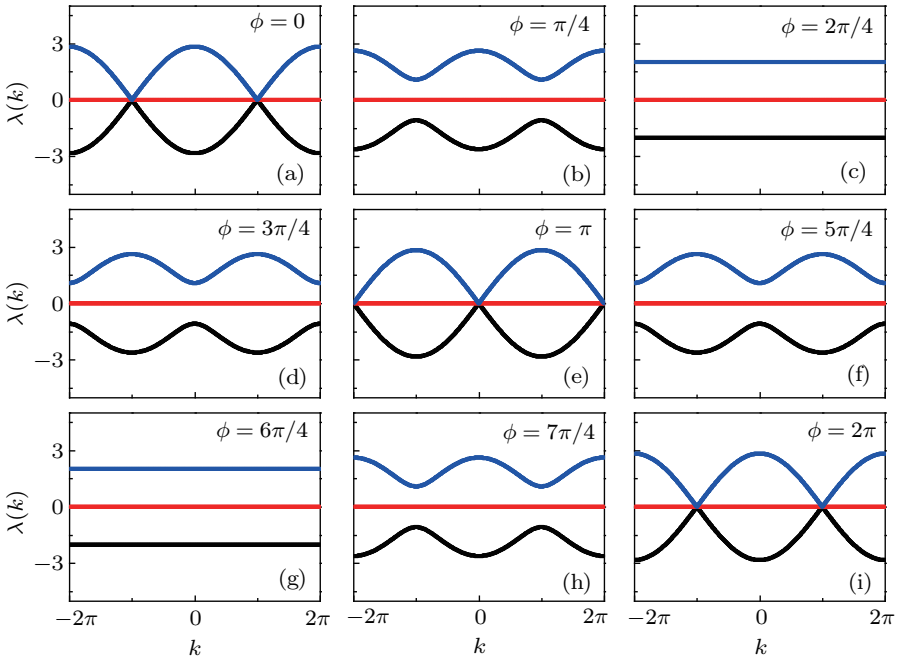


Fig. 3. (color online) Same as in Fig. 2, but for different synthetic magnetic flux ϕ with vertical tilting $\varepsilon_{\text{v}} = 0$.

Figure 3 demonstrates the effect of the artificial magnetic flux ϕ on the energy levels for the system with $\varepsilon_{\text{v}} = 0$. In the absence of ϕ ($\phi = 0$), energy bands cross at $k = \pm\pi$ when horizontal tilting $\varepsilon_{\text{h}} = 0$ (see Fig. 3(a)). The energy levels λ_+ (blue line) and λ_- (black line) are gradually far away from flat band λ_{flat} (red line) as the increase of ϕ ($\phi = \pi/4$ in Fig. 3(b)). However, λ_+ (blue line) and λ_- (black line) also become flat band when $\phi = \pi/2$, i.e., there are three flat bands ($\lambda_{\text{flat}} = 0$, $\lambda_{\pm} = \pm 2$) when $\phi = \pi/2$ as shown in Fig. 3(c), whose CLS is as Eq. (10). However, as the further increase of ϕ (see Fig. 3(d)

and 3(e)), two of the three flat bands disappear while the energy bands are closed at $k = 0, \pm 2\pi$. As the further increase of ϕ, the gaps are re-opened and three flat bands re-occur when $\phi = 3\pi/2$, and finally, the gaps are closed at $k = \pm\pi$ when $\phi = 2\pi$ (the energy bands of $\phi = 0$ are recovered). Note that the crossing of energy levels exists with $\phi = 0$, $\phi = \pi$, and $\phi = 2\pi$ while there are three flat bands with $\phi = \pi/2$ and $\phi = 3\pi/2$, whose CLS is as Eq. (10). Interestingly, the values of k at which the energy bands cross depend on ϕ, which will result in different tunneling dynamics.

4. Tunneling dynamics

When $\varepsilon_{\rm h} \neq 0$, we find that, intriguing and significant phenomena occur in the diamond lattice chain, including Landau–Zener tunneling, Bloch oscillations, and localization phenomenon, which skips different ranges of lattice sites in a single chain or among different chains. Vertical tilting $\varepsilon_{\rm v}$ and artificial magnetic flux ϕ may change the energy gap and alter the energy band structure, enforcing the occurrence of Landau–Zener tunneling, which scans the whole Bloch bands. The transition among Landau–Zener tunneling, Bloch oscillations, and localization phenomenon is not only closely related to the characters of the energy bands, but also depends on the initial configuration of the bosons in the diamond lattice chain. In order to reveal the rich tunneling dynamics for bosons in the diamond lattice chain, we set the initial configuration of bosons as various linear combinations of the CLS as Gaussian wavepacket, i.e., $\{a_n, b_n, c_n\} \sim {\rm e}^{-n^2/2\sigma^2}$, where $\varepsilon_{\rm h} = 0.05$, $\sigma = 10$ invariably. The tunneling dynamics is demonstrated by the space–time evolution of the total norm density $p_n(t) = |a_n|^2 + |b_n|^2 + |c_n|^2$ for bosons, whose corresponding evolution in single chain (a, b, and c chains) are depicted by $|a_n(t)|^2$, $|b_n(t)|^2$, and $|c_n(t)|^2$, respectively.

4.1. The effect of vertical tilting

In the absence of horizontal tilting $\varepsilon_{\rm h}$ ($\varepsilon_{\rm h} = 0$), the effect of vertical tilting $\varepsilon_{\rm v}$ on the energy levels has already been investigated with $\phi = 0$ in Fig. 3(a) ($\varepsilon_{\rm v} = \phi = 0$) and Fig. 2 ($\phi = 0$ but $\varepsilon_{\rm v} \neq 0$), and here we study the counterparts of the tunneling dynamics for bosons with various initial configurations when horizontal tilting $\varepsilon_{\rm h} = 0.05$ and artificial magnetic flux $\phi = 0$.

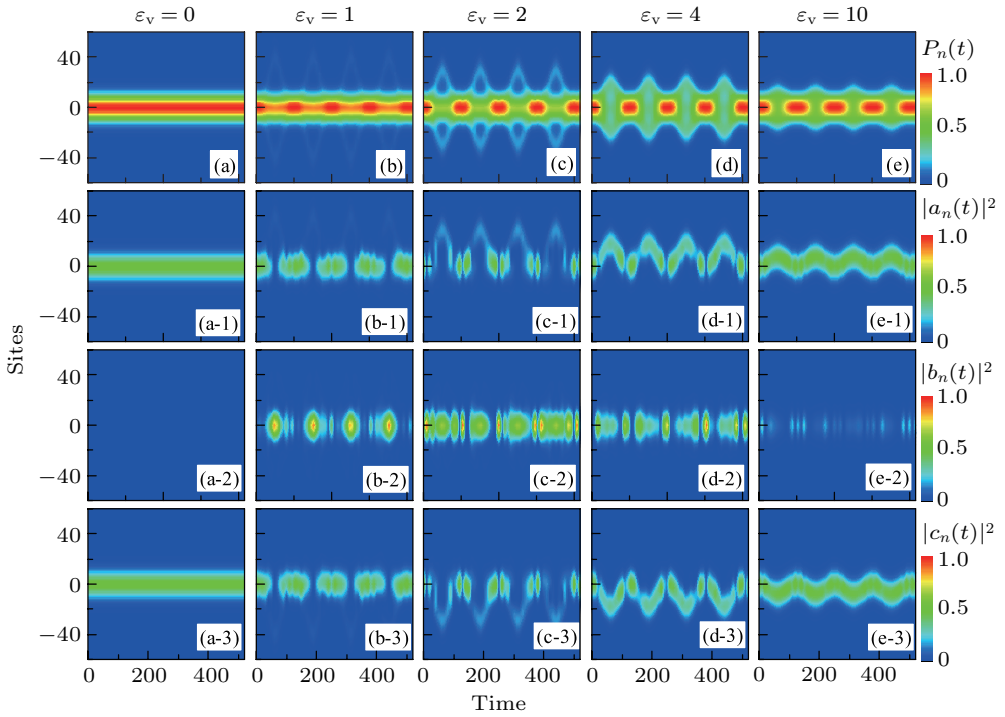


Fig. 4. (color online) The effect of vertical tilting $\varepsilon_{\rm v}$ on the tunneling dynamics for bosons initially configured as $\{a_n, b_n, c_n\} = \{1, 0, -1\}\,{\rm e}^{-n^2/2\sigma^2}$ (the eigenstate for the case of $\phi = \varepsilon_{\rm v} = 0$), which is demonstrated by the space–time evolution of the norm density $p_n(t)$ (the first row) and the corresponding evolution for bosons in single chain (a, b, and c chains) are depicted by $|a_n(t)|^2$ (the second row), $|b_n(t)|^2$ (the third row), and $|c_n(t)|^2$ (the fourth row), respectively.

When bosons are initially distributed as the eigenstate $\{a_n, b_n, c_n\} = \sqrt{1/2}\{1, 0, -1\}\,{\rm e}^{-n^2/2\sigma^2}$ for CLS with flat band $\lambda_{\rm flat} = 0$, the effect of $\varepsilon_{\rm v}$ on the tunneling dynamics for bosons with this initial configuration in the diamond lattice chain is investigated with $\phi = 0$, which is demonstrated in Fig. 4. In the absence of $\varepsilon_{\rm v}$ ($\varepsilon_{\rm v} = 0$), the energy levels for the system cross at $k = \pm\pi$, bosons maintain their initial CLS, i.e., bosons are equationally distributed in a and c chains of the diamond lattice chain (see the first column in Fig. 4). However, in the presence of $\varepsilon_{\rm v}$ ($\varepsilon_{\rm v} \neq 0$), the energy gap occurs and the structure of energy band may alter qualitatively in Fig. 2, so is the counterpart of tunneling dynamics for bosons in the diamond

lattice chain. With small ε_v ($\varepsilon_v = 1$), weak Bloch oscillations occur along the positive direction of lattice sites in a chain and the negative direction in c chain, which are antisymmetric, demonstrated by $p_n(t)$ in Fig. 4(b) and further illustrated by the corresponding $|a_n(t)|^2$ in Fig. 4(b-1) and $|c_n(t)|^2$ in 4(b-3), respectively. What is interesting is that the evolution of $|b_n(t)|^2$ in Fig. 4(b-2)) is nonzero as the progress in time, i.e., the exchange of bosons among a, b, and c chains exists, which indicates the occurrence of Landau–Zener tunneling as well as the transition from the localization phenomenon to Landau–Zener tunneling and weak Bloch oscillations. For medium ε_v ($\varepsilon_v = 2$), Bloch oscillations in a (c) chain of the diamond lattice chain are heightened (see the third column in Fig. 4). The increasing number of bosons in b chain (see Fig. 4(c-2)) further implies the transition from localization phenomenon to Landau–Zener tunneling and Bloch oscillations. That transition is induced by a partial constructive interference of wave functions for a, b, and c chains with the increase of ε_v. Note that the counterpart of energy bands for the system with $\varepsilon_v = 2$ can be seen from Fig. 2(b), where the energy levels are rising and the gaps between the adjacent energy bands are broadened. As a consequence, Landau–Zener tunneling, Bloch oscillations, and localization phenomenon are coexisting simultaneously. With the appropriate ε_v ($\varepsilon_v = 4$), the range of lattice sites for Bloch oscillations in a and c chains shrinks. However, the bosons number in both a and c chain increases while it is reduced in b chain (see in Figs. 4(d), 4(d-1), 4(d-2), and 4(d-3)), which stands for the harvest of localization phenomenon from Landau–Zener tunneling and Bloch oscillations gradually in the diamond lattice chain, whose energy levels are shown in Fig. 2(c), where the energy levels are rising and the gaps between the adjacent energy bands are broadened sequentially. Significantly, three flat bands ($\lambda_{\text{flat}} = 0$, $\lambda_{\pm} = \pm\varepsilon_v$) hold when ε_v is large enough ($\varepsilon_v = 10$) in Fig. 2(d), whose tunneling dynamics for bosons in the diamond lattice chain is illustrated in the fifth column of Fig. 4. Note that there almost exists no bosons in b chain (see Fig. 4(e-2)). We find that, the transition from Landau–Zener tunneling as well as Bloch oscillations to localization phenomenon holds, i.e., localization phenomena are harvested completely from Landau–Zener tunneling as well as Bloch oscillations. Consequently, the tunneling dynamics for bosons initially configured as $\{a_n, b_n, c_n\} = \sqrt{1/2}\{1, 0, -1\}\,\mathrm{e}^{-n^2/2\sigma^2}$ (CLS) experiences a nonlinear transition process among a, b, and c chains with the increase of ε_v in Figs. 4(a), 4(b), 4(c), 4(d), and 4(e). Interestingly, the Bloch oscillations in b chain have never happened.

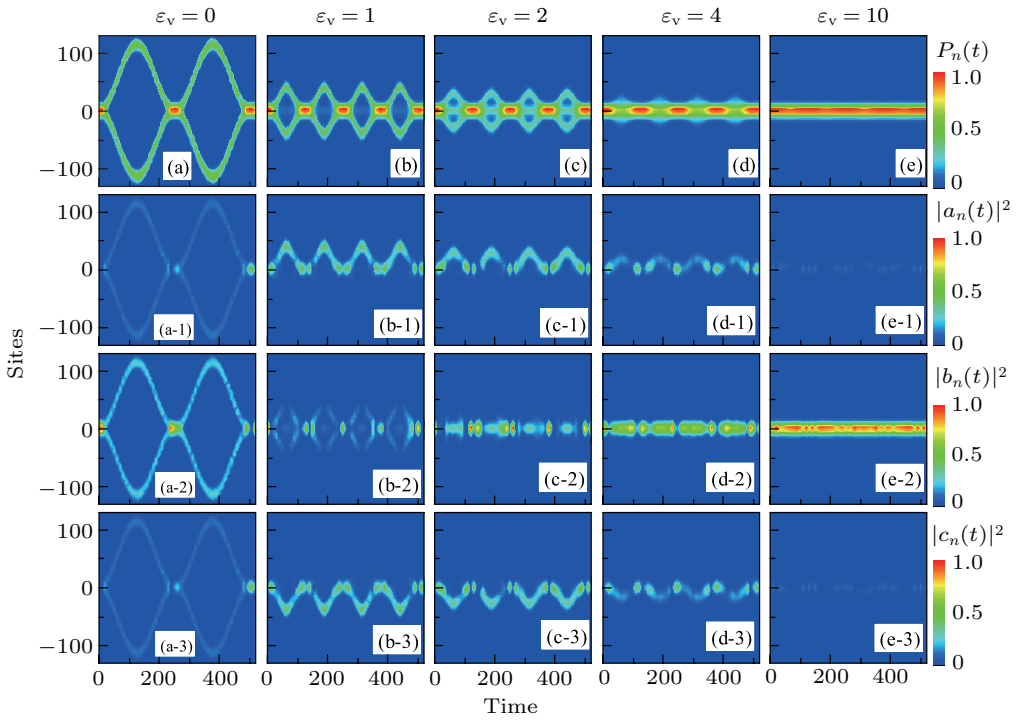


Fig. 5. (color online) The same as that in Fig. 4, but for the initial configuration of bosons in the diamond chain as $\{a(t), b(t), c(t)\} = \{0, 1, 0\}\,\mathrm{e}^{-n^2/2\sigma^2}$ (not the eigenstate).

Providing the initial configuration of bosons as the linear combination with the states given by Eq. (8) when $\varepsilon_v = 0$ at $k = 0$, i.e., $\{a(t), b(t), c(t)\} = \{0, 1, 0\}\,\mathrm{e}^{-n^2/2\sigma^2}$ (not the eigenstate), that is, bosons only exist in b chain while no boson exist in a and c chains at $t = 0$, the effect of ε_v on the tunneling dynamics for bosons in the diamond lattice chain is investigated with $\phi = 0$, which is demonstrated in Fig. 5. In the absence of ε_v ($\varepsilon_v = 0$, see the first column in Fig. 5), the energy levels cross at $k = \pm\pi$ (see Fig. 3(a)), bosons do perfect symmetrical bidirectional bloch oscillations with a large range (−125th

to 125th) along the direction of lattice site in the three chains, except for the predominant bosons in b chain, i.e., Landau–Zener tunneling occurs within bloch oscillations. However, in the presence of ε_v ($\varepsilon_v \neq 0$), an energy gap occurs (see Fig. 2), and the counterpart of tunneling dynamics for bosons in the diamond lattice chain exhibited intriguing phenomena, including Landau–Zener tunneling, Bloch oscillations, and localization phenomenon. With small ε_v ($\varepsilon_v = 1$), the original range for Bloch oscillations (-125th to 125th in Fig. 5(a)) along the direction of the lattice site experiences a big shrinkage and the frequencies of the Bloch oscillations are doubled (see Fig. 5(b)). Besides, the symmetrical bidirectional bloch oscillations in a and c chains for $\varepsilon_v = 0$ in Fig. 5(a) transform into nonreversing bloch oscillation in a (along the positive direction of lattice sites) and c (along the negative direction of lattice sites) chain with the increase of ε_v, which are antisymmetric and exhibited in Figs. 5(b-1), 5(b-2), and 5(b-3), where the number of bosons in a and c chains increases predominantly while it decreases significantly in b chain, indicating that appropriate ε_v may promote the occurrence of Landau–Zener tunneling. Note that Landau–Zener tunneling and Bloch oscillations are coexisting in the diamond lattice chain. With moderate ε_v ($\varepsilon_v = 2$, see the third column in Fig. 5), the nonreversing Bloch oscillations in a and c chains (antisymmetric) are weakened slightly while the bidirectional bloch oscillations in b chain are suppressed in the first place accompanying with the occurrence of localization phenomenon. The coexistence of Landau–Zener tunneling, Bloch oscillations, and localization phenomenon holds in the diamond lattice chain when $\varepsilon_v = 2$. With the further increasing ε_v ($\varepsilon_v = 4$, see the fourth column in Fig. 5), the energy gap becomes wider and the nonreversing Bloch oscillations in a and c chains are enormously suppressed while the localization phenomenon in b chain are enhanced tremendously. That indicates localization phenomenon are almost harvested from Landau–Zener tunneling and Bloch oscillations. When ε_v is large enough ($\varepsilon_v = 10$), the energy bands become three flat bands in Fig. 2(d), which gives rise to the transition from Landau–Zener tunneling and Bloch oscillations to localization phenomenon completely (see the fifth column in Fig. 5), i.e., bosons almost are completely localized in b chain. Consequently, when bosons are initially configured as $\{a_n, b_n, c_n\} = \{0,1,0\}\mathrm{e}^{-n^2/2\sigma^2}$ in the diamond lattice chain, the tunneling dynamics experiences a damping evolution process induced by ε_v.

In brief, intriguing and significant phenomena occur in the diamond lattice chain, including Landau–Zener tunneling, Bloch oscillations, and localization phenomenon, which skips different ranges of lattice sites in single chain or among different chains. Vertical tilting ε_v may alter the energy bands structure, changing the Landau–Zener tunneling which scans the whole Bloch bands. The transition among Landau–Zener tunneling, Bloch oscillations, and localization phenomenon, can be affected significantly by the structure of the energy bands as well as the initial configuration of the bosons in the diamond lattice chain.

4.2. The effect of artificial magnetic flux

When vertical tilting $\varepsilon_v = 0$, the tunneling dynamics still exhibits the transition and the coexistence of Landau–Zener tunneling, Bloch oscillations, and localization phenomenon, which can be induced by artificial magnetic flux ϕ ($\phi \neq 0$) and similar to that in Figs. 4 and 5. However, the structure of energy bands can be altered by ϕ ranging from 0 to π, i.e., when $0 \leq \phi < \pi/2$, the minimum band gap for the crossing occurs around $k = \pm\pi$ while it is at $k = 0$ approximately in the case of $\pi/2 < \phi \leq \pi$, which is demonstrated by the energy levels in Fig. 3. Three flat bands exist on the condition that $\phi = \pi/2$. The novel phenomena of tunneling dynamics are just induced by altering the structure of energy levels.

Figure 6 illustrates the effect of artificial magnetic flux ϕ on the tunneling dynamics for bosons with the same initial configuration as that in Fig. 4, i.e., $\{a_n, b_n, c_n\} = \{1,0,-1\}\mathrm{e}^{-n^2/2\sigma^2}$. As $0 < \phi < \pi/2$, the tunneling dynamics mainly manifest as Landau–Zener tunneling among three chains, where a small number of bosons do weak bloch oscillations in b chain while the majority of bosons are localized in a and c chains. A large number of bosons exist in b chain with $\phi = \pi/2$, which indicates the enhancement of Landau–Zener tunneling among a, b, and c chains, where the weak oscillations in each chain disappear and almost all bosons are localized around the 0th lattice site, which is well coincident with the three flat bands ($\phi = \pi/2$, see Fig. 3(c)). When $\pi/2 < \phi < \pi$, the tunneling dynamics, principally, exhibits complicated Landau–Zener tunneling among three chains and Bloch oscillations in each chain. More interestingly, the Bloch oscillations in a and c chains are asymmetric. Given $\phi = \pi$, the system is degraded to the eigenstate and bosons maintain its initial CLS. That is, the energy levels $\lambda_\pm$ of the system experience nonlinear transitions from dispersion structure to flat band and then come back to dispersion structure again when ϕ ranges from 0 to π, which makes the tunneling dynamics complicated.

It is illustrated in Fig. 7 that the tunneling dynamics for bosons with the same initial configuration as that in Fig. 5, i.e., $\{a(t), b(t), c(t)\} = \{0,1,0\}\mathrm{e}^{-n^2/2\sigma^2}$. The tunneling dynamics is basically consistent before ($0 < \phi < \pi/2$) and after ($\pi/2 < \phi < \pi$) the transition of the energy band structure (dispersion structure or flat band), which is similar to that in Fig. 6 ($\pi/2 < \phi < \pi$). Furthermore, the tunneling dynamics for the system recovers to Bloch oscillations entirely with $\phi = \pi$, whose range of lattice sites is reduced by half compared with that in the case of $\phi = 0$. The range of lattice sites and oscillation frequency of Bloch oscillations are affected by ϕ ($0 < \phi < \pi$).

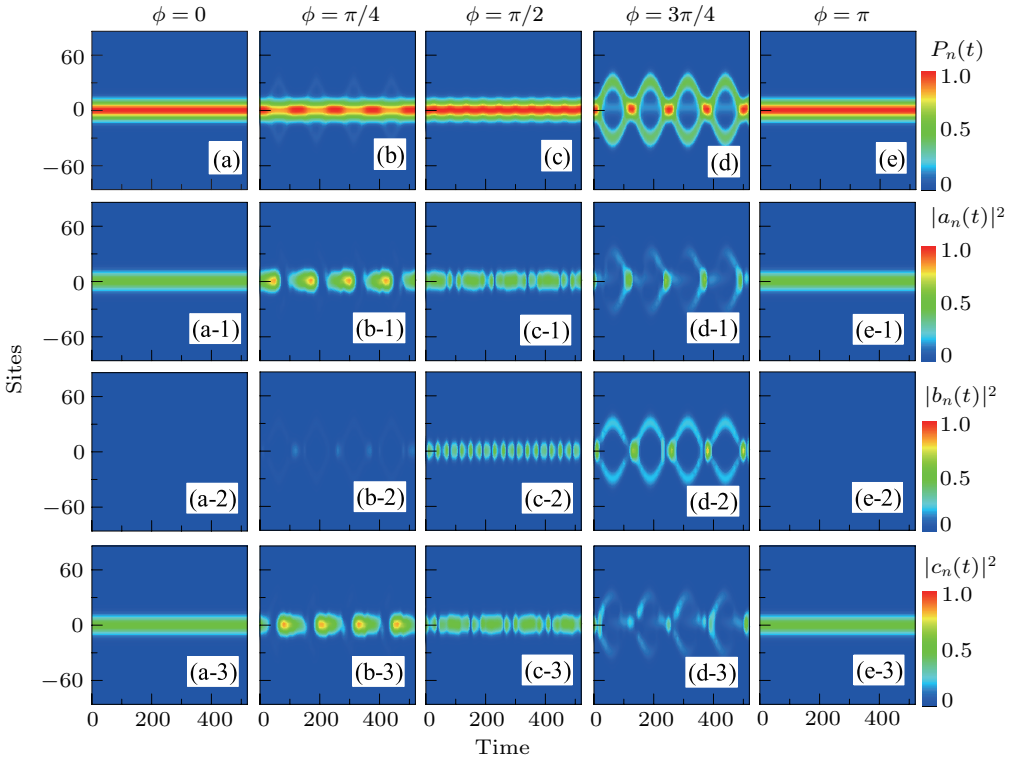


Fig. 6. (color online) The effect of artificial magnetic flux ϕ on the tunneling dynamics for bosons initially configured as $\{a_n, b_n, c_n\} = \{1, 0, -1\}\, e^{-n^2/2\sigma^2}$ (the eigenstate for the case of $\phi = \varepsilon_v = 0$), which is demonstrated by the space–time evolution of the norm density $p_n(t)$ (the first row) and the corresponding evolution for bosons in single chain (a, b, and c chains) are depicted by $|a_n(t)|^2$ (the second row), $|b_n(t)|^2$ (the third row), and $|c_n(t)|^2$ (the fourth row), respectively.

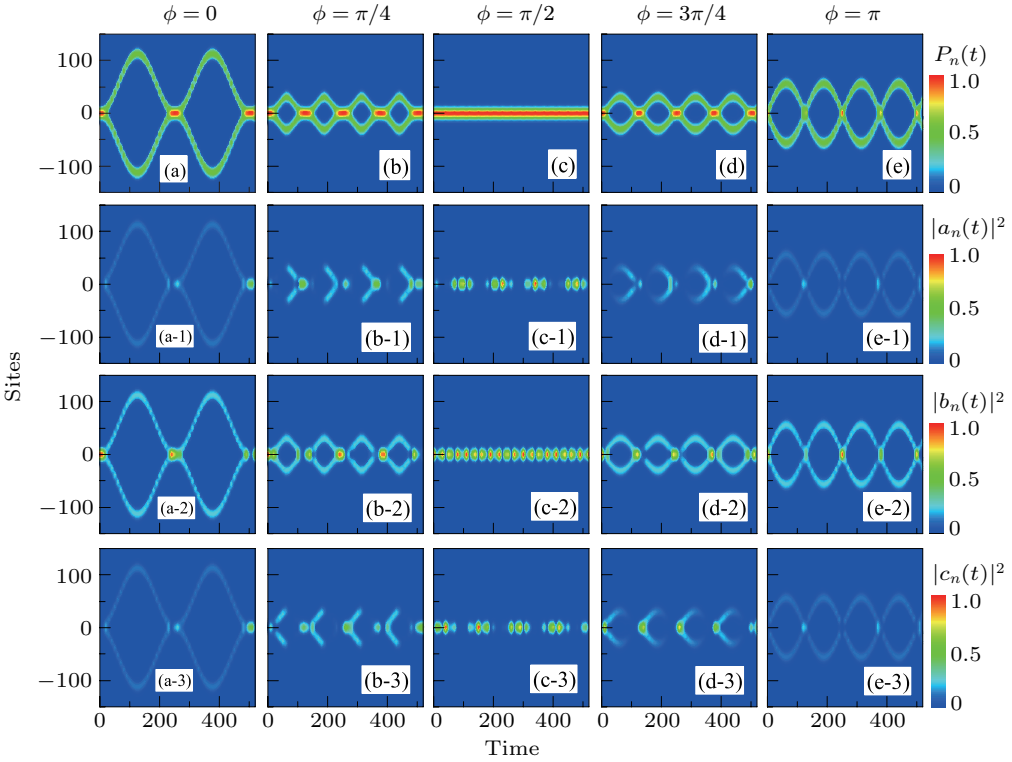


Fig. 7. (color online) The same as in Fig. 6, but for the initial configuration of bosons in the diamond chain as $\{a(t), b(t), c(t)\} = \{0, 1, 0\}\, e^{-n^2/2\sigma^2}$ (not the eigenstate).

Figures 6–7 further prove that the tunneling dynamics for the system is closely related to artificial magnetic flux ϕ, which also depends on the initial configuration of bosons in the diamond lattice chain. In order to further illustrate this, figure 8 gives the tunneling dynamics for bosons configured as $\{a(t), b(t), c(t)\} = \{1, -1, 1\}\, e^{-n^2/2\sigma^2}$ (not the eigenstate) initially. Interestingly, the Bloch oscillations in three chains are nonreversing and the directions of the Bloch oscillations are opposite before ($\phi < \pi/2$)

and after ($\phi > \pi/2$) the transition of the energy band structure. More interestingly, the Bloch oscillations become bidirectional when $\phi = \pi$, whose range of the lattice sites is reduced by half while the oscillation frequencies are doubled, compared with that in the case of $\phi = 0$. The range of lattice sites and oscillation frequency for Bloch oscillations are affected by ϕ ($0 < \phi < \pi$).

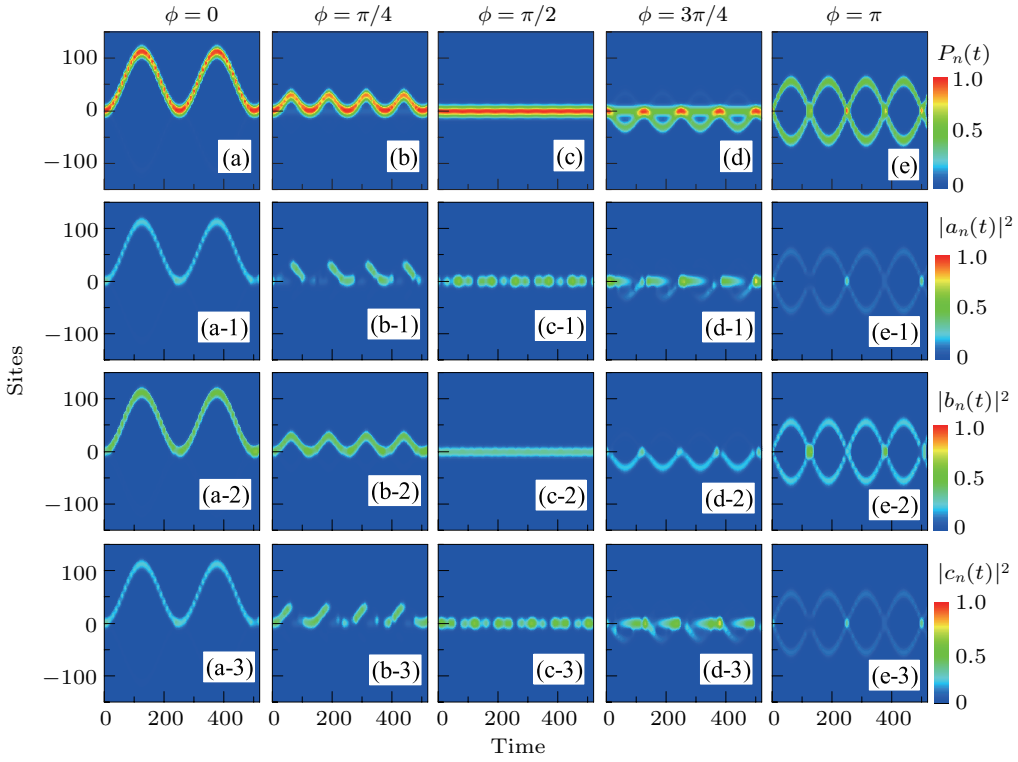


Fig. 8. (color online) The same as in Fig. 6, but for the initial configuration of bosons in the diamond chain as $\{a(t), b(t), c(t)\} = \{1, -1, 1\}\, e^{-n^2/2\sigma^2}$ (not the eigenstate).

In a word, artificial magnetic flux ϕ can alter the structure of energy levels for the system, making it possible to manipulate the transitions among Landau–Zener tunneling, Bloch oscillations, and localization phenomenon, which also depend on the initial configuration of the bosons in the diamond lattice chain.

5. Conclusion

It is proved in this paper that both vertical tilting and artificial magnetic flux can alter the position of the minimum band gap for the crossing, inducing intriguing and significant phenomena for bosons with various initial configurations in the diamond lattice chain, including Landau–Zener tunneling, Bloch oscillations, and localization phenomenon, among which the transitions are not only closely related to the structure of the energy bands for the system (dispersion structure or flat band), but also depend on the initial configuration of bosons in the diamond lattice chain. As a consequence, Landau–Zener tunneling, Bloch oscillations, and localization phenonmenon of bosons always counteract and are complementary with each other in the diamond lattice chain.

Understanding the mechanism of tunneling dynamics for bosons in the diamond lattice chain with tilting and artificial magnetic flux can contribute to designing some atomic devices, i.e., atom switch, for selective transport concerning a definite number of bosons among diverse sites and chains. Furthermore, our study could stimulate the investigations of quantum dynamics in the presence of a nonlinear term and even be extended to multi-shape lattice systems, such as, triangle, square, and pentagram lattices. As a result, this engineering may provide a quantitatively theoretical foundation for precise manipulation of bosons in experiments.

References

[1] Juliá D B, Dagnino D, Lewenstein M, Martorell J and Polls A 2010 *Phys. Rev. A* **81** 023615
[2] Chatterjee B, Brouzos I, Cao L and Schmelcher P 2012 *Phys. Rev. A* **85** 013611
[3] Zhu Q, Zhang Q and Wu B 2015 *J. Phys. B: At. Mol. Opt. Phys.* **48** 045301
[4] Chang N N, Yu Z F, Zhang A X and Xue J K 2017 *Chin. Phys. B* **26** 115202
[5] Morsch O, Müller J H, Cristiani M, Ciampini D and Arimondo E 2001 *Phys. Rev. Lett.* **87** 140402
[6] Jona M L, Morsch O, Cristiani M, *et al.* 2003 *Phys. Rev. Lett.* **91** 230406
[7] Konotop V V, Kevrekidis P G and Salerno M 2005 *Phys. Rev. A* **72** 023611
[8] Loladze V, Khomeriki R 2017 *Phys. Rev. E* **95** 042204
[9] Anderson M H, Matthews M R, Wieman C E and Cornell E A 1995 *Science* **269** 198
[10] Anderson B P and Kasevich M A 1998 *Science* **282** 1686
[11] Schmitt J, Damn T, Dung D, Vewinger F, Klaers J and Weitz M 2014 *Phys. Rev. Lett.* **112** 030401

[12] Trombettoni A and Smerzi A 2001 *Phys. Rev. Lett.* **86** 2353
[13] Cazalilla M A, Citro R, Giamarchi T, Orignac E and Rigol M 2011 *Rev. Mod. Phys* **83** 1405
[14] Spreeuw R J C, Druten N J, Beijersbergen M W, Eliel E R and Woerdman J P 1990 *Phys. Rev. Lett.* **65** 2642
[15] Bouwmeester D, Dekker N H, Dorsselaer F E V, Schrama C A, Visser P M and Woerdman J P 1995 *Phys. Rev. A* **51** 646
[16] Wu B and Niu Q 2000 *Phys. Rev. A* **61** 023402
[17] Liu J, Fu L, Ou B Y, Chen S G, Choi D I, Wu B and Niu Q 2002 *Phys. Rev. A* **66** 023404
[18] Chen Y A, *et al.* 2011 *Nat. Phys.* **7** 61
[19] Asamitsu A, Tomioka Y, Kuwahara H and Tokura Y 1997 *Nature* **388** 50
[20] Miyano K, Tanaka T, Tomioka Y and Tokura Y 1997 *Phys. Rev. Lett.* **78** 4257
[21] Yamanouchi S, Taguchi Y and Tokura Y 1999 *Phys. Rev. Lett.* **83** 5555
[22] Oka T and Aoki H 2005 *Phys. Rev. Lett.* **95** 137601
[23] Sugimoto N, Onoda S and Nagaosa N 2008 *Phys. Rev. B* **78** 155104
[24] Cristiani M, Morsch O, Müller J H, Ciampini D and Arimondo E 2002 *Phys. Rev. A* **65** 063612
[25] Jona-Lasinio M, Morsch O, Cristiani M, Malossi N, Müller J H, Courtade E, Anderlini M and Arimondo E 2003 *Phys. Rev. Lett.* **91** 230406
[26] Struck J, OĬschlağer C, Weinberg M, Hauke P, Simonet J, Eckardt A, Lewenstein M, Sengstock K andWindpassinger P 2012 *Phys. Rev. Lett.* **108** 225304
[27] Zheng Y, Feng S P and Yang S J 2017 *Phys. Rev. A* **96** 063613
[28] Zheng Y, Feng S P and Yang S J 2018 *Phys. Rev. A* **97** 043627
[29] Lopes A A and Dias R G 2011 *Phys. Rev. B* **84** 085124
[30] Rojas O, Souza D S M and Ananikian N S 2012 *Phys. Rev. E* **85** 061123
[31] Khomeriki R and Flach S 2016 *Phys. Rev. Lett* **116** 245301
[32] Zegadlo K, Dror N and Hung N V 2017 *Phys. Rev. E* **96** 012204
[33] Ramachandran A, Andreanov A and Flach S 2017 *Phys. Rev. B* **96** 161104
[34] Nguyen Hong-Son and Tran Minh-Tien 2016 *Phys. Rev. B* **94** 125106
[35] Derzhko O, Richter J and Maksymenko M 2015 *Int. J. Mod. Phys. B* **29** 1530007